

The role of superficial geology in controlling groundwater recharge in the weathered crystalline basement of semi-arid Tanzania

E. Zarate^{a,b,*}, D. Hobley^a, A.M. MacDonald^b, R.T. Swift^{b,c}, J. Chambers^b, J. J. Kashaigili^d, E. Mutayoba^e, R.G. Taylor^f, M.O. Cuthbert^{a,g,h}

^a School of Earth & Environmental Sciences, Cardiff University, Main Building, Park Pl, Cardiff CF10 3AT, UK

^b British Geological Survey, Lyell Centre, Research Av South, Edinburgh EH14 4AP, UK

^c University of Liege, Urban and Environmental Engineering, 4000 Liege, Belgium

^d Sokoine University of Agriculture, P.O. Box 3013, Morogoro, Tanzania

^e Water Institute, Water Resources Department, PO Box 35059, Dsm, Tanzania

^f Department of Geography, University College London, London, WC1E 6BT, UK

^g The University of New South Wales (UNSW), School of Civil and Environmental Engineering, Sydney, Australia

^h Water Research Institute, Cardiff University, Cardiff, CF10 3AT, UK

ARTICLE INFO

Keywords:

Groundwater recharge
Conceptual model
Superficial geology
Semi-arid
Hydrogeology
Focused recharge

ABSTRACT

Study region: Little Kinyasungwe River Catchment, central semi-arid Tanzania.

Study focus: The structure and hydraulic properties of superficial geology can play a crucial role in controlling groundwater recharge in drylands. However, the pathways by which groundwater recharge occurs and their sensitivity to environmental change remain poorly resolved. Geophysical surveys using Electrical Resistivity Tomography (ERT) were conducted in the study region and used to delineate shallow subsurface stratigraphy in conjunction with borehole logs. Based on these results, a series of local-scale conceptual hydrogeological models was produced and collated to generate a 3D conceptual model of groundwater recharge to the wellfield.

New hydrological insights for the region: We propose that configurations of superficial geology control groundwater recharge in dryland settings as follows: 1) superficial sand deposits act as collectors and stores that slowly feed recharge into zones of active faulting; 2) these fault zones provide permeable pathways enabling greater recharge to occur; 3) 'windows' within layers of smectitic clay that underlie ephemeral streams may provide pathways for focused recharge via transmission losses; and 4) overbank flooding during high intensity precipitation events increases the probability of activating such permeable pathways. These conceptual models provide a physical basis to improve numerical models of groundwater recharge in drylands, and a conceptual framework to evaluate strategies (e.g., Managed Aquifer Recharge) to artificially enhance the availability of groundwater resources in these regions.

* Corresponding author at: School of Earth & Environmental Sciences, Cardiff University, Main Building, Park Pl, Cardiff CF10 3AT, UK.
E-mail address: zaratee@cardiff.ac.uk (E. Zarate).

<https://doi.org/10.1016/j.ejrh.2021.100833>

Received 1 February 2021; Received in revised form 4 May 2021; Accepted 11 May 2021

Available online 24 May 2021

2214-5818/© 2021 Published by Elsevier B.V. This is an open access article under the CC BY-NC-ND license

(<http://creativecommons.org/licenses/by-nc-nd/4.0/>).

1. Introduction

Drylands (subhumid to hyper-arid regions) cover 45 % of the earth's surface (Prävälíe, 2016) and support a population of around 2 billion people, 90 % of whom live in developing countries (UN, 2017). Characterized by large atmospheric water demands and temperature contrasts (Cherlet et al., 2018), surface water is often seasonally or perennially absent in drylands (Wheater et al., 2008) and groundwater is often the principal and most reliable source of water in these regions (MacDonald et al., 2012; Shanafield and Cook, 2014).

Owing to their hydrological characteristics, drylands are likely to experience increased water stress in the coming decades (Gleeson et al., 2012; Taylor, 2014; Wada et al., 2010) due to anthropogenic pressures (Chen et al., 2019; DESA, 2017; Rulli et al., 2013; Wada et al., 2013) and climatic changes (Abel et al., 2020; Berdugo et al., 2020; Huang et al., 2017; Taylor et al., 2013a). Hence, improved understanding and quantification of groundwater recharge in dryland areas is critical to the sustainable management of groundwater resources in the future (Gleeson et al., 2020; Head et al., 2014; Meixner et al., 2016).

Groundwater recharge in drylands often occurs by way of leakage from runoff and surface-water sources, a process we refer to in this paper as 'focused recharge' (Simmers, 2003; Healy and Scanlon, 2010; Cuthbert et al., 2016, 2019a, 2019b). Yet, despite its present and future importance, the spatio-temporal controls on focused groundwater recharge in drylands, and their sensitivity to environmental change, are currently poorly understood (Acworth et al., 2016; Cuthbert et al., 2019a; Scanlon et al., 2006; Taylor et al., 2013a; Wheater et al., 2010).

In temperate climates, the geometry and permeability of superficial deposits is known to moderate potential recharge to underlying bedrock aquifers (Griffiths et al., 2011; Misstear et al., 2009), and local-scale configurations of these deposits provide recharge pathways through high permeability layers (Cuthbert et al., 2009). It is also likely that the structure and hydraulic properties of superficial geology play a crucial role in controlling surface-groundwater interactions in drylands (Scanlon et al., 2006; Wheater et al., 2010). For example, marked temporal and spatial variability in the hydraulic conductivities of streambed and floodplain deposits can provide controls on surface-groundwater interactions in dryland ephemeral stream systems (Costa et al., 2012; Dahan et al., 2008; Flinchum et al., 2020; McCallum et al., 2014; Telvari et al., 1998; Wang et al., 2017). Further, heterogeneities in the hydraulic properties and structure of superficial deposits have been hypothesised to influence the subsurface dynamics of groundwater recharge to deeper aquifers (Acworth et al., 2020; Rau et al., 2017).

Few studies to date have made quantitative detailed observations of superficial geological structure in drylands to better understand the likely flowpaths and processes controlling groundwater recharge. The objectives of this paper are thus to explore the potential physical basis for groundwater recharge by determining the geometry and inter-relationships between superficial deposits, underlying geology, and fracture systems in the intensively monitored and pumped groundwater system of the Makutapora Wellfield in the Little Kinyasungwe River Catchment of central Tanzania. This system comprises a weathered and fractured crystalline basement aquifer system that is overlain in part by low permeability smectitic clays and, despite intensive groundwater abstraction, is replenished on a decadal timescale by episodic recharge events (Taylor et al., 2013b). To accomplish this, we conducted a series of geophysical investigations using Electrical Resistivity Tomography (ERT) and, in conjunction with borehole data and field observations, identified various geoelectrical structures and correlated these with interpreted subsurface lithology. Based on these findings, we present a series of local- and basin-scale conceptual models that identify multiple potential recharge pathways, illustrating how superficial geology may control focused recharge in the Little Kinyasungwe River Catchment. Although our study was not designed to quantitatively determine the relative proportions of diffuse and focused recharge in the Little Kinyasungwe River Catchment, our conceptual models provide a first step in quantifying recharge in the study area in the future, and we propose these models will be transferable to other dryland regions globally.

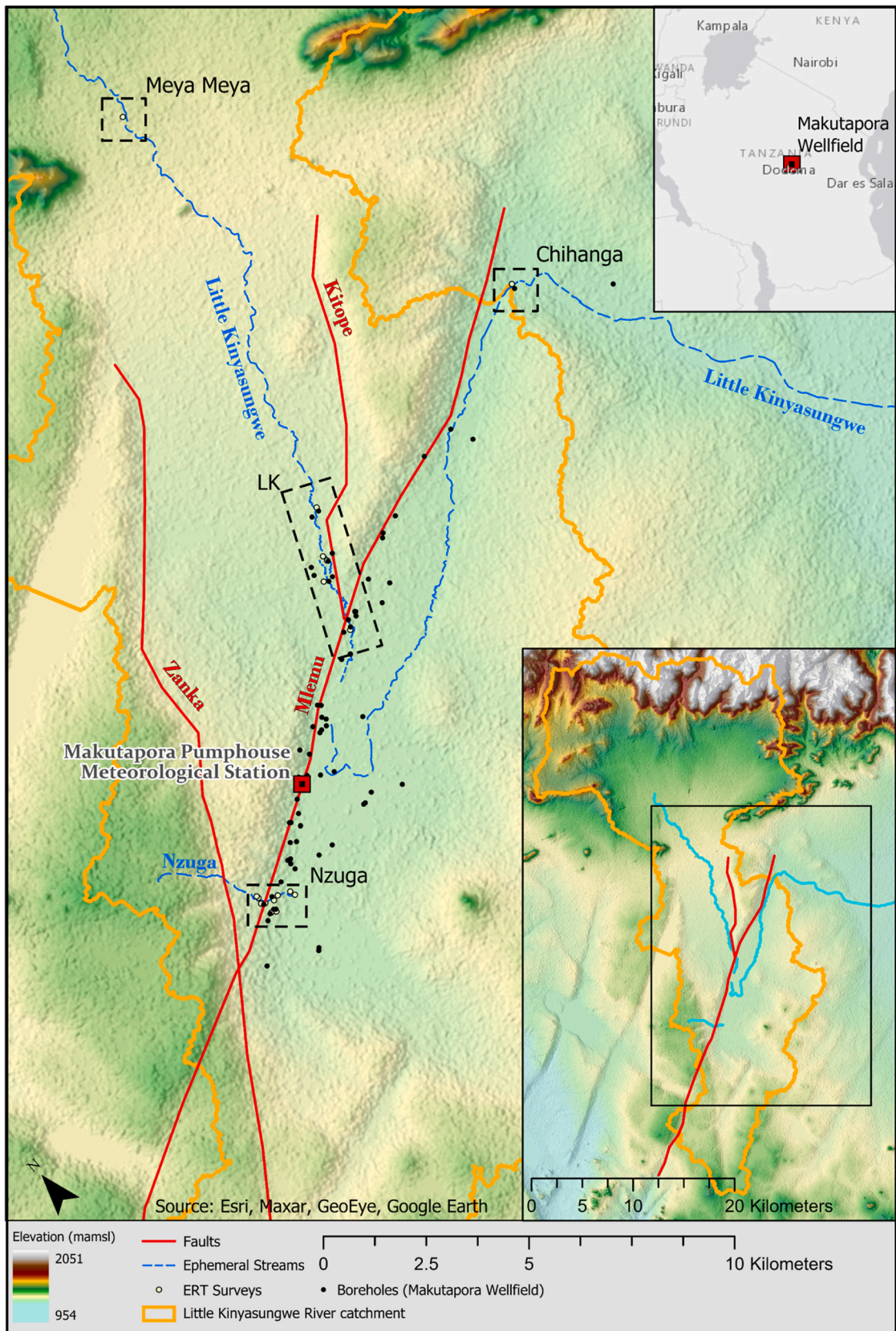
2. Materials and methods

2.1. Study area

The Makutapora Wellfield, situated within the Little Kinyasungwe River Catchment (Fig. 1), is underlain by the fractured crystalline basement of the Dodoma craton in central Tanzania (Kashaigili et al., 2003) and is approximately 20 km north of the capital city, Dodoma. The catchment occupies an area of 698 km² upstream of the Chihanga flow gauge located (Fig. 1) at the catchment outlet and forms the upper section of the River Wami Basin. (Shindo, 1989).

The climate is semi-arid and characterized by distinct wet and dry seasons. Average air temperatures are 23 °C, with highs ranging from 26.5 °C to 30.5 °C in July-October, and lows from 13.6 °C to 18.8 °C in Nov-June (WMO, 2020). Average annual precipitation is 550 mm at Makutapora Meteorological Station (Fig. 1), 99 % of which falls in a single wet season from December to April (Seddon, 2019; Taylor et al., 2013b). Short-lived observations in the catchment suggest that precipitation in the upland areas may be greater than on the floor of the catchment (Onodera et al., 1995; Seddon et al., 2021). There have been several estimates of potential evapotranspiration in Makutapora (Fawley, 1958; Kashaigili et al., 2003; Onodera et al., 1995; Shindo, 1989, 1990), the most recent being 2120 mm·yr⁻¹, based on 3 non-consecutive years of data recorded between 2003 and 2006 at the Makutapora Meteorological Station (Seddon, 2019).

The catchment is underlain by basement rocks comprised of Precambrian synorogenic granites and migmatite biotite gneiss of the Dodoma Basement Superterrane (De Pauw et al., 1983; Kabete et al., 2012; Ministry of Water, 1976), with more intrusive ultrabasic complexes of amphibolite and quartzo-feldspathic gneisses with biotite outcropping within the wellfield and Meya Meya regions (Fig. 1). Metamorphosed rocks are also present in the region and amphibole schists crop out in a belt of inselbergs surrounding Meya



(caption on next page)

Fig. 1. The Makutapora Wellfield with NASA Shuttle Radar Topography Mission data (30 m resolution) Digital Elevation Model (NASA et al., 2019) overlain. Location of study sites outlined in black and location of wellfield within greater Little Kinyasungwe River catchment (inset). Catchment was delineated using the Digital Elevation Model (DEM). Major faults in the study area are labelled and name and position as mapped by current literature (Rwebugisa, 2008; Shindo, 1990).

Meya (Julian et al., 1963).

Apart from outcrops at the topographic highs of the Chenene Hills (Kashaigili, 2010) or along channels of ephemeral streams (Hayashi and Chiba, 1994), these basement rocks are generally covered by a deeply weathered regolith (50–100 m thick) of fractured saprock, saprolite, and pedolitic products of Neogene age at varying stages of chemical decomposition (Julian et al., 1963). Regolith composition varies throughout and is related to the mineralogy of the underlying parent rock.

The regolith is overlain by unconsolidated alluvial material consisting of detrital sands, gravels, and silts. (Kashaigili et al., 2003; Nkotagu, 1996). In the centre of the catchment and in the lowland areas of the wellfield depression, the regolith is overlain by layers of black, smectitic 'Mbuga' clay (Onodera et al., 1995). Such black smectitic clays often exist as valley infill in the rifted basins of central Tanzania (Bianconi and Borshoff, 1984). These are also typical of other semi-arid regions across the world in similar geological contexts (Oakes and Thorp, 1951), and have previously been associated with the presence of seasonal freshwater swamps in Makutapora (Wade and Oates, 1938).

Tectonic activity associated with the Manyara-Dodoma rift segment, a branch of the East African Rift system extending south across the Dodoma craton (Dawson, 2008), has left a complex network of faults in the study area. These faults are expressed as linear features trending SW-NE & NW-SE across the topography of the region (Macheyeki et al., 2008) as seen in Fig. 1. The main faults that cross the study area, the Mlemu and Kitope, form a natural NW boundary to the Makutapora wellfield, which is situated along a distinct fault-bounded topographic lowland depression within the wider catchment, and there is evidence of further faulting north of the catchment (Kabete et al., 2012). The large-scale discontinuities and dense fracture networks associated with faults such as the Mlemu are the defining hydrogeological feature of Makutapora, giving rise to anomalously high transmissivities of 400 to 4000 m²d⁻¹ within the wellfield, and producing high well yields in boreholes proximal to the faults (Maurice et al., 2019; Rwebugisa, 2008).

The wellfield is presently the sole source of Dodoma's municipal and industrial water supply and in 2016 supplied the city with an average of 50,000 m³·day⁻¹ of freshwater (DUWASA, 2017). Groundwater abstraction in the wellfield has increased from 0.1 to 1.5 million m³ per month and, despite having exceeded previous estimates of its maximum sustainable yield, groundwater levels are currently higher than they were in the 1990s and roughly the same as they were prior to development (Seddon, 2019). Long-term groundwater level data from the wellfield indicates that intensive groundwater abstraction is replenished on a decadal timescale by episodic recharge events during exceptional seasonal rainfalls associated with El Niño events, interrupting multi-annual recessions in groundwater levels (Cuthbert et al., 2019b; Kolusu et al., 2019; Taylor et al., 2013b).

Previous research in the catchment suggests that this episodic recharge is focused by way of ephemeral streams flowing over coarse-grained soils within alluvial fans at the margins of the wellfield depression (Onodera et al., 1995; Shindo, 1989, 1990). Diffuse recharge through the soil matrix or via soil macropores and fractures that bypass the soil matrix, is also thought to occur within the catchment (Shindo, 1989, 1990). However, it is not known what the relative contributions of diffuse and focused recharge are in this area, nor is it addressed quantitatively in this study.

2.2. Geophysical methods

2.2.1. Electrical resistance tomography data acquisition, processing, and inversion

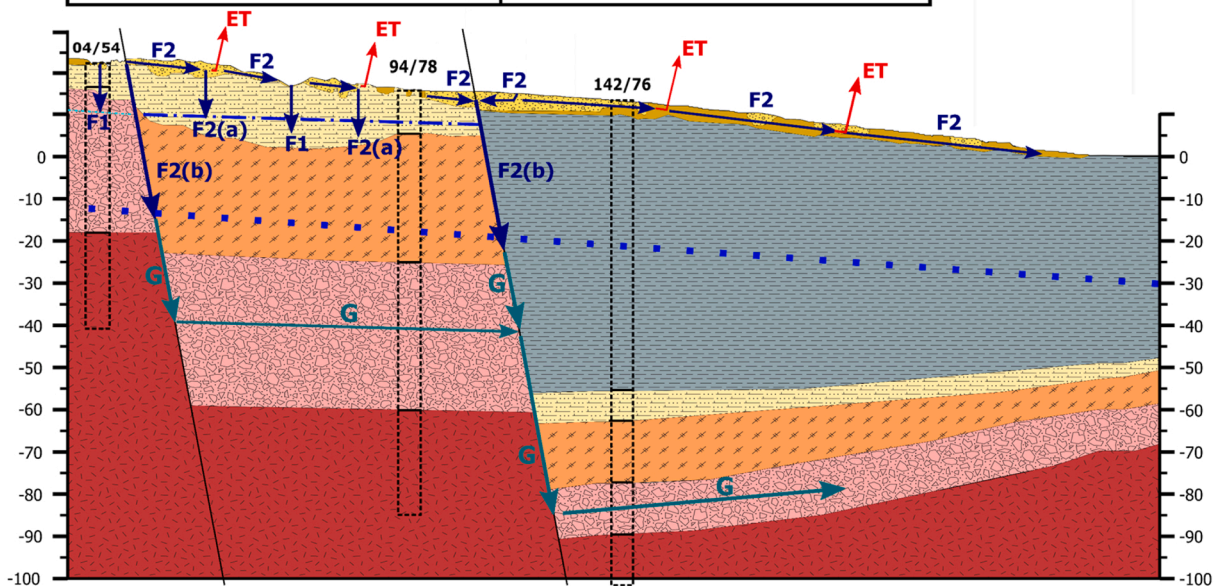
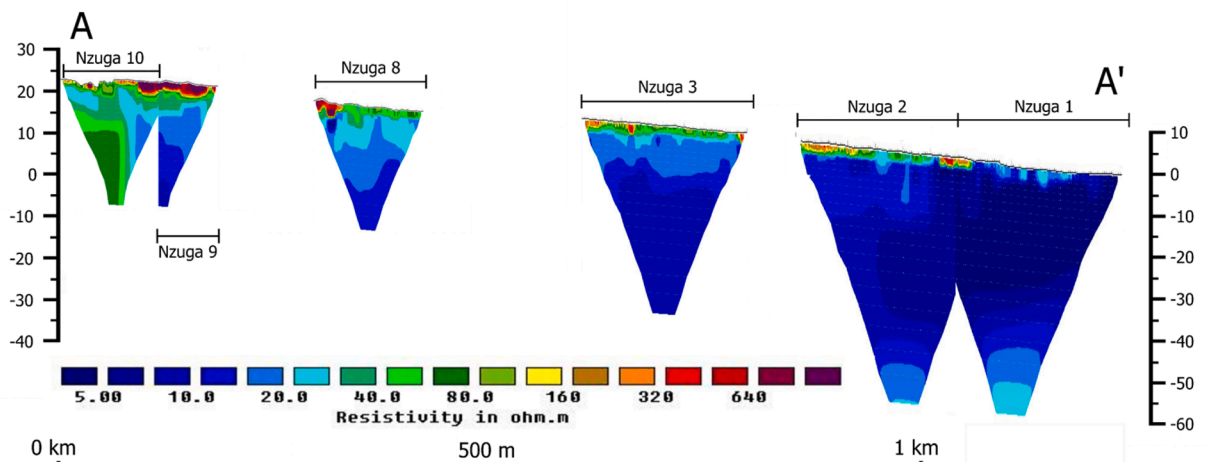
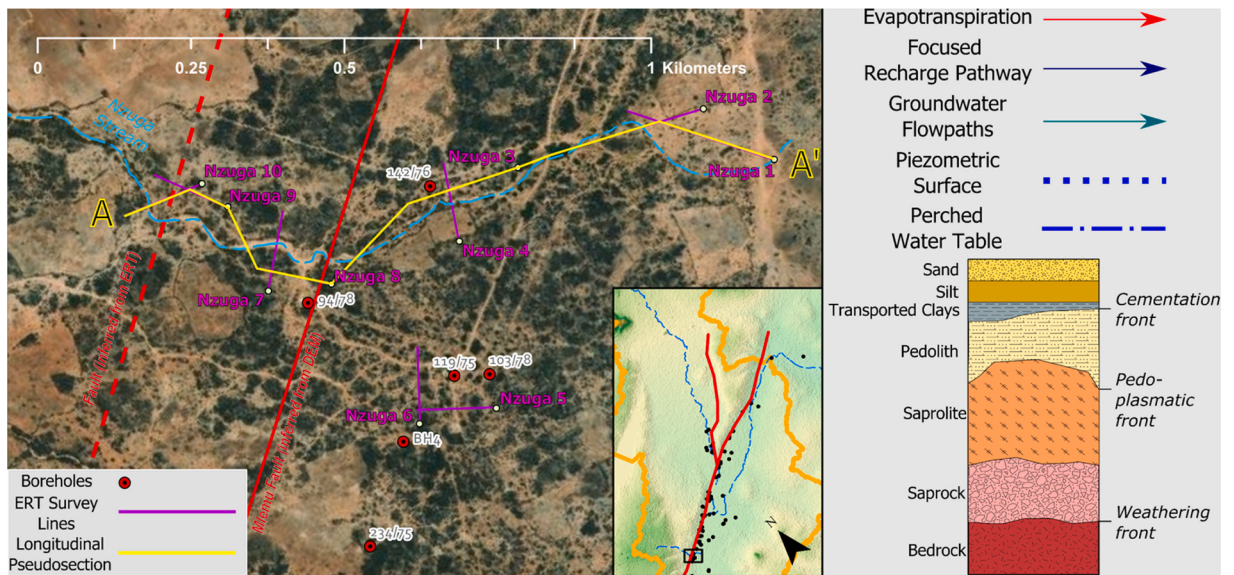
Geophysical techniques have received increasing attention in recent years due to their non-destructive character and ability to provide information on subsurface features over large areas (Binley et al., 2015; Parsekian et al., 2015; Singha, 2017). Among the available techniques, electrical resistivity tomography (ERT) was chosen for this study for its ability to map and characterise superficial deposits for hydrological interpretation (e.g. Gourry et al., 2003; Andersen and Acworth, 2009; Cuthbert et al., 2009; Clifford and Binley, 2010; Gourdol et al., 2018).

In this study an AGI SuperSting R8 resistivity meter (<http://www.agiusa.com>) was used in dipole-dipole configuration. This configuration made efficient use of the instrument's multichannel capability and provided good lateral and vertical resolution. A 64-electrode array with dipole sizes (a) of a = 6 and a = 8, and dipole separations (n*a) with n = 1–8 were used, and combinations of long (>3 m) electrode spacings used in areas where penetration depth was important, while shorter (2 m) electrode spacings used in areas where high resolution targets were to be delineated (see Table S1 for detailed survey set-up parameters)

Areas close to and parallel with roads or overhead power cables were avoided to minimize interference from other electrical signals or man-made disturbances of the subsurface. Dry and hard-ground conditions necessitated the use of saltwater to improve electrode contact resistance, and scrub vegetation commonly had to be removed to ensure the lines were able to maintain precise, straight-line orientations. Start and end points of sections were located using a GPS (Garmin eTrex 10) to <5 m uncertainty and orientated by taking a compass bearing. The relative elevations of the topographic variations along each line were measured using a Leica Disto D410 with a vertical accuracy of 1 mm.

Each apparent resistivity measurement was made in normal ρ_n and reciprocal ρ_r configuration (LaBrecque et al., 1996) with the measurement value used defined as the mean of these two measurements, ρ_m . The percentage standard error in this mean, referred to here as the reciprocal error, e , is defined as:

$$|e| = 100 \cdot \left(\frac{|\rho_r - \rho_n|}{(\rho_r + \rho_n)} \right) \quad (1)$$



(caption on next page)

Fig. 2. Nzuga study site - with map of ERT surveys (top), combined longitudinal geoelectric section of the study site (middle) and interpreted geological structure and conceptual model (bottom). Interpreted borehole logs (Table A2) superimposed in black. Labels and arrows drawn correspond to recharge pathways outlined in in Section 3.2.

Negative apparent resistivity data points were removed, and measurements with reciprocal errors greater than 5% were filtered out. This filtered dataset was inverted using the RES2DINV (Geotomo Software) algorithm (Loke, 2001). A least squares data constraint was used that minimizes the error between the observed and calculated apparent resistivity values, and a limit of 4 iterations was set to avoid model over-fitting. A robust model constraint, incorporating topographic variations, was selected over a least squared inversion constraint since it is known to better resolve sharp geological boundaries expected within the study area (Loke et al., 2003). In this case, it was important to delineate the boundaries between the superficial deposits, in-situ regolith, and zones bounded by normal faulting. Inverted data are presented as geoelectric pseudosections (Edwards, 1977) and used in the interpretation of geoelectric layers and subsurface lithology.

2.2.2. Interpretation of geoelectrical models

Due to the smoothing and non-uniqueness inherent in fitting 3D geological structure to 2D resistivity models (Aizebeokhai and Singh, 2013; Dahlin et al., 2007), independent data were used to aid interpretation and to assist in identifying layer boundaries in the images. Boreholes with lithological data proximal to survey lines were collated from the Tanzanian Ministry of Water in Dodoma (Table A2) and superimposed onto these sections to correlate geoelectrical layers and lithological observations. In addition, field observations were used to constrain the resistivity ranges for superficial deposits observed at the ground surface. Sharp discontinuities seen in the geoelectrical sections were corroborated with field observations of faulted zones and regions of faulting inferred from analysing topographical data from STRM 30 m DEM of the study area (NASA et al., 2019).

Water content and temperature variations are known to affect subsurface resistivity (Brunet et al., 2010) but these effects were not considered in the interpretation of geological layers since they are greatly outweighed by contrasts in resistivity due to lithological variation, which are the focus of this study. Further, geophysical surveys were undertaken in the middle of the dry season (June-July) when variations in soil moisture content and temperature between the dates of individual surveys were minimal.

Forward modelling using the RES2DMOD software (Loke, 2002) was used to identify and rule out various unexpected features found in some of the inversions to decide whether they should be interpreted as ‘true’ variations in subsurface resistivity. Firstly, several inversions at the Nzuga (Figs. A4, 9–12), LK (Fig. A15, 17), Meya Meya (Fig. A18) and Chihanga (Fig. A19) sites show low resistivity zones underlying regions of high ($> 250 \Omega \text{ m}$) resistivity at the surface. Secondly, we observe many sections at Nzuga (Figs. A9–11) and Meya Meya sites (Fig. A19) which have decreasing resistivity with depth underlying shallower zones of $> 40 \Omega \text{ m}$ resistivity (See Section 3.1 for further discussion).

Using the field site profile characteristics of the Nzuga 8 survey (Fig. A10), a simplified two-layer synthetic model of the subsurface was developed for the forward modelling exercise. The top layer for the model was defined as 0–2.5 m with a resistivity of $40 \Omega \text{ m}$, and the bottom layer from 2.5 to 30 m with a resistivity of $20 \Omega \text{ m}$ (Fig. A20). Two regions 10 m wide and 3 m thick with high, $1000 \Omega \text{ m}$ resistivities were then added to the model to examine the effects of pockets of high resistivity material (Fig. A21). The synthetic results indicate that these low resistivity features (circled in black in Fig. A21) occur despite the attempts to minimise the number of iterations and are thus anomalous features. Further synthetic results indicate that sections with decreasing resistivity with depth were indeed true features that cannot be re-created without adding decreasing resistivity layers with depth in our forward models.

2.3. Survey locations

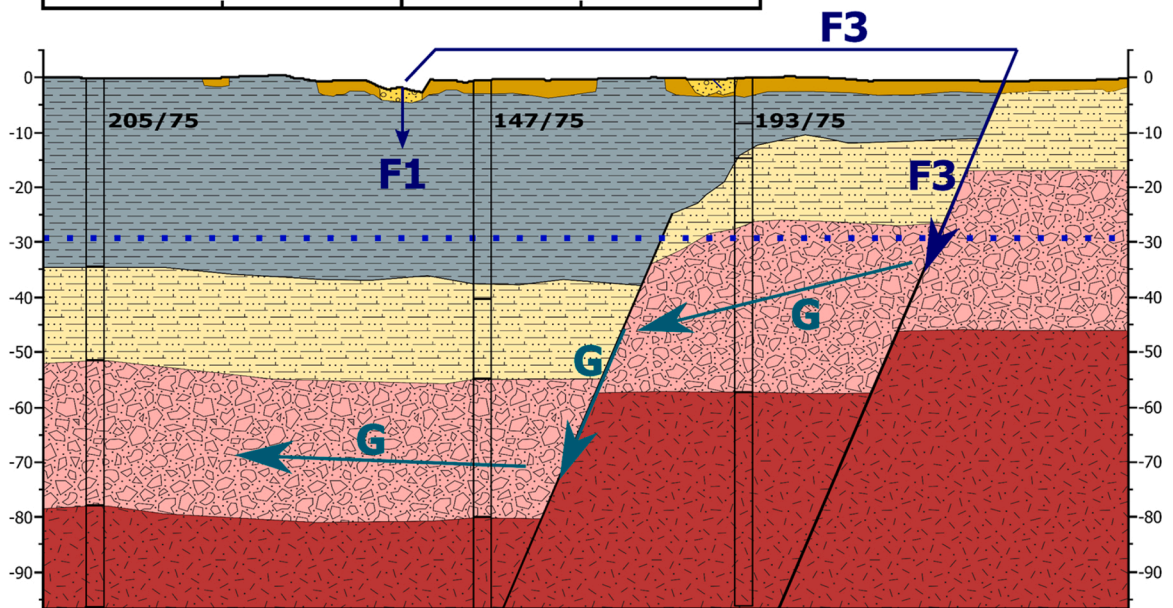
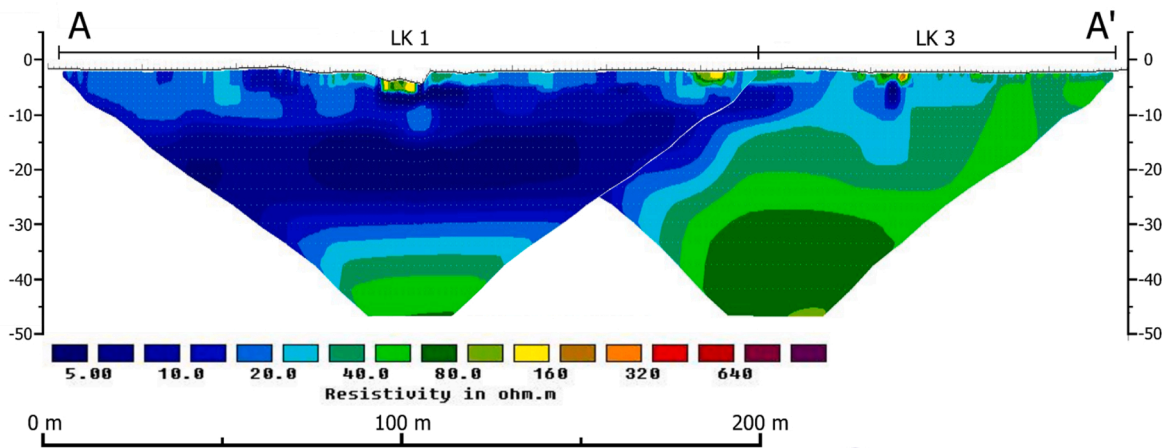
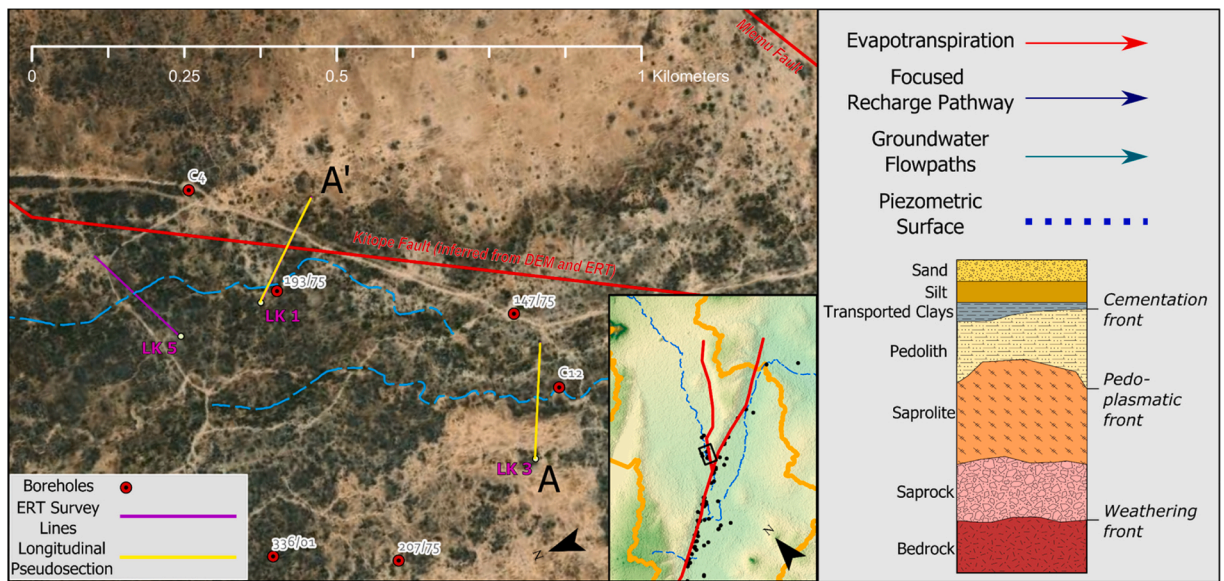
A total of 17 ERT surveys were conducted in June and July 2019 at four locations within the study area. These areas are shown in Fig. 1, and a map of survey lines at each study site are shown inset within Figs. 2–5. These locations were chosen to be representative of the various catchment areas that surround the wellfield as described for each site below. Three sites (Meya Meya, LK and Chihanga) are situated on the Little Kinyasungwe River, which comprises 75 % of the catchment area draining into the Makutapora wellfield depression.

Meya Meya, the furthest upstream survey site, is located approximately 20 km upstream from the Makutapora wellfield. This location was chosen for one survey (Fig. 6 and A18) to coincide with the long-term stream gauge monitoring taking place at the site (Seddon et al., 2021). This gauge measures the inflow of the Little Kinyasungwe River into the next downstream study site (LK). The purpose of surveys in this area is to provide geological context to streamflow patterns recorded here and the geological structure comprising upland ‘pediplain’ areas that surround the wellfield (Shindo, 1989).

The site ‘LK’ was chosen for 5 surveys (Figs. A13–17) to constrain the geological configuration underneath the Little Kinyasungwe River as it enters the wellfield depression. This site is bounded by the Kitope fault to the East and is situated in a lowland area covered by Mbuga Clay and silts. In seasons with particularly high precipitation, these lowland regions can experience overland flow and inundation during the wet season (Fig. A2).

The Chihanga site represents the furthest downstream survey site on the Little Kinyasungwe River and was chosen for one survey (Fig. 5 and A19). Like Meya Meya, it was chosen to constrain the geological conditions as the stream exits the wellfield depression into the downstream Hombolo basin.

The fourth site is in the vicinity of the ephemeral Nzuga stream and lies on the North-Western edge of the wellfield. This site was chosen for 10 surveys (Fig. 2 and A3–12). The Nzuga stream crosses the Zanka and Mbuga faults before terminating in the wellfield



(caption on next page)

Fig. 3. LK study site - with map of ERT surveys (top), combined longitudinal geoelectric section of the study site (middle) and interpreted geological structure and conceptual model (bottom). Interpreted borehole logs (Table A2) superimposed in black. Labels and arrows drawn correspond to recharge pathways outlined in in Section 3.2.

depression, forming an alluvial fan. Spot gauging within the stream has shown that ephemeral streamflow does not always reach the depression and is instead thought to be lost by leakage from the stream channel into underlying and surrounding superficial deposits (Shindo, 1990). Such ‘headwater channels’ (Sutfin et al., 2014) are common throughout the region in the transition slopes between upland and lowland areas and comprises approximately 25 % of the catchment area flowing into the catchment.

3. Results and discussion

3.1. Geoelectric units

Integrating the results of the 17 ERT surveys (Figs. A3–19) with interpreted borehole log information (Table A2) and outcrop field observations (Fig. A1), we defined five main geoelectrical units in the catchment, and associated inferred lithologic properties and depositional settings as follows:

- a) Deposits of coarse sand ($>250 \Omega \text{ m}$) and silts (20–160 $\Omega \text{ m}$)
- b) Transported smectitic clays ($<10 \Omega \text{ m}$)
- c) Cemented pedolitic soils (30–80 $\Omega \text{ m}$)
- d) Smectite-rich Saprolite (15–30 $\Omega \text{ m}$)
- e) Weathered saprock (110–450 $\Omega \text{ m}$)

These layers correspond to the idealised weathering profile of tropical soils above crystalline basement rocks described in the literature (Dewandel et al., 2006; Fookes, 1997; Taylor and Eggleton, 2001; Taylor and Howard, 1999; Wright and Burgess, 1992) and fall within a corresponding range of resistivities for weathered products of mafic origin containing 2:1 clays established for similar geological provinces (Anudu et al., 2014; Barongo and Palacky, 1991; Beauvais et al., 1999; Belle et al., 2019; Ritz et al., 1999; Robineau et al., 2007). The presence or absence of the different layers in the profile varies from location to location in the study area, which we interpret due to local variations in rock type and structure, topography and rates of sediment erosion and deposition.

The topmost layer (a) comprises sand of variable grain sizes ranging from coarse to fine (See Fig. A1 3c) with resistivities $>250 \Omega \text{ m}$, set amongst silts with resistivities of 20–160 $\Omega \text{ m}$. Sand is 0.5–4 m thick and is present but often discontinuous at all the study sites. Continuous $<0.5 \text{ m}$ thick layers of sand were directly observed within the dry streambeds of the Nzuga (Figs. A6, 9, 12), and Little Kinyasungwe River at Meya Meya (Fig. A18), LK (Figs. A15, 17) and Chihanga (Fig. A19). Thicker layers of sand are particularly prominent at the Nzuga site, where they exist as 1–4 m thick deposits in and around the banks of the Nzuga (Figs. A5, 9–12), and smaller 1–2 m thick deposits in Little Kinyasungwe (Figs. A15, 17). Owing to their channel-like morphology, we interpret these sand deposits as abandoned ephemeral stream channel alluvial deposits. Silts often surround these pockets of coarser alluvium and are most commonly present as $<0.5 \text{ m}$ thin layers in the soil profile surrounding the Nzuga stream and Little Kinyasungwe River. However, thicker layers (1–2 m) of these silts are particularly prominent in the alluvial fan of the Nzuga (Figs. 3, A3, 4), and in the floodplain areas surrounding the Little Kinyasungwe River at the LK site (Figs. 4, A13, 15, 17, and see Fig A1 5). We interpret these as overbank deposits from the existing or previous ephemeral stream network.

Very low resistivity layers ($<10 \Omega \text{ m}$) (b) are present in every study area, and in outcrops that correspond with layers of black, smectitic ‘Mbuga Clay’ (see Fig. A1 4). This clay layer is 30 m thick in the downstream reaches of the Nzuga stream where it meets the wellfield depression

(Figs. 3 and A3–5) and is also present as a 10–25 m thick layer below the Little Kinyasungwe River in the LK site (Figs. 4 and A15–17). At the Meya Meya site, this low resistivity clay exists only as an isolated 0.5 m thick layer 40 m away from the Little Kinyasungwe River (Fig. A19). More prominent 0.5–1 m thick deposits of this clay can be seen surrounding but not underlying the Little Kinyasungwe River at the Chihanga site (Figs. 5 and A19). We interpret these clay layers to be transported basin infill deposits in the downthrown side of Mlemu and Kitope faults at the Nzuga and LK sites, respectively. However, at Chihanga it is unclear whether these deposits are previous basin infill that has subsequently been cut through by the Little Kinyasungwe, or more recent over bank deposits.

Underlying these transported sediments, we observe a zone of approximately 80 $\Omega \text{ m}$ (c) that crops out within the Nzuga streambed (see Fig. A1 3b) but only upstream of the Mlemu Fault (Figs. 3 and A11–12), as well as within the streambed of the Little Kinyasungwe River at both the Meya Meya (see Fig. A1 1a) and Chihanga sites. This comprises quartz grains (1–4 mm) interbedded in a yellow to white fine sandy-clay matrix (see Fig. A1 3a). At the Nzuga (Figs. 3 and A9–12) and Meya Meya (Fig. A18) sites, the resistivity of this zone further decreases with depth, from approximately 80 to 30 $\Omega \text{ m}$. Comprising the uppermost in-situ cemented layer of our profile, we interpret this layer as a pedolith (or mottled zone), with a decrease in resistivity with depth suggesting a transition from 1:1 pedogenic clays to increasing proportion of 2:1 clays

as the weathering profile moves below the water table and approaches the saprolite (Pal et al., 1989). This transition is common in tropical profiles, and in the partial weathering of mafic materials, where 2:1 clays typically persist below the water table where less intense weathering processes in the saturated zone inhibits weathering of 2:1 clays to kaolinite (Taylor and Howard, 1999). At

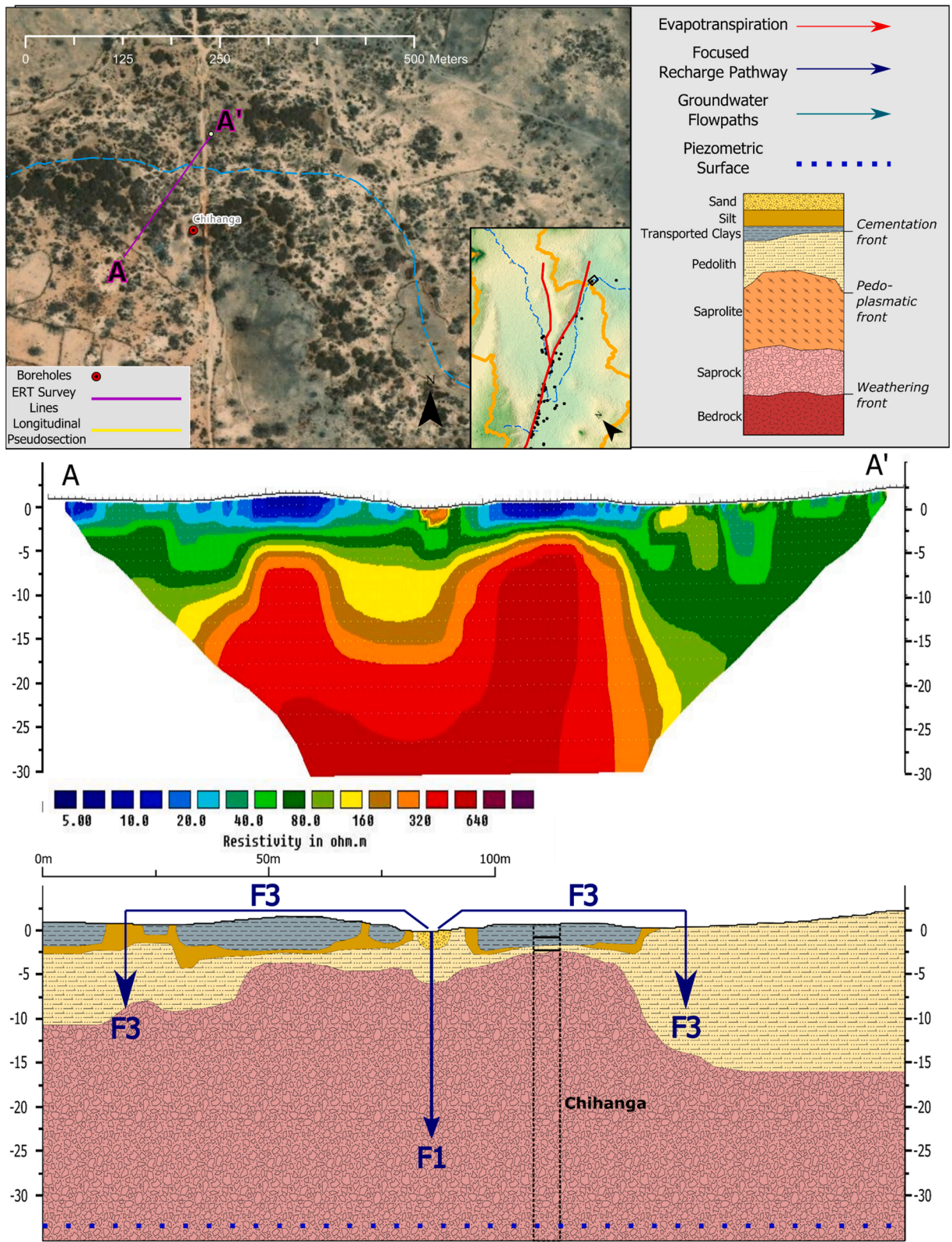


Fig. 4. Chihanga study site - with map of ERT surveys (top), combined longitudinal geoelectric section of the study site (middle) and interpreted geological structure and conceptual model (bottom). Interpreted borehole logs (Table A2) superimposed in black. Labels and arrows drawn correspond to recharge pathways outlined in in Section 3.2.

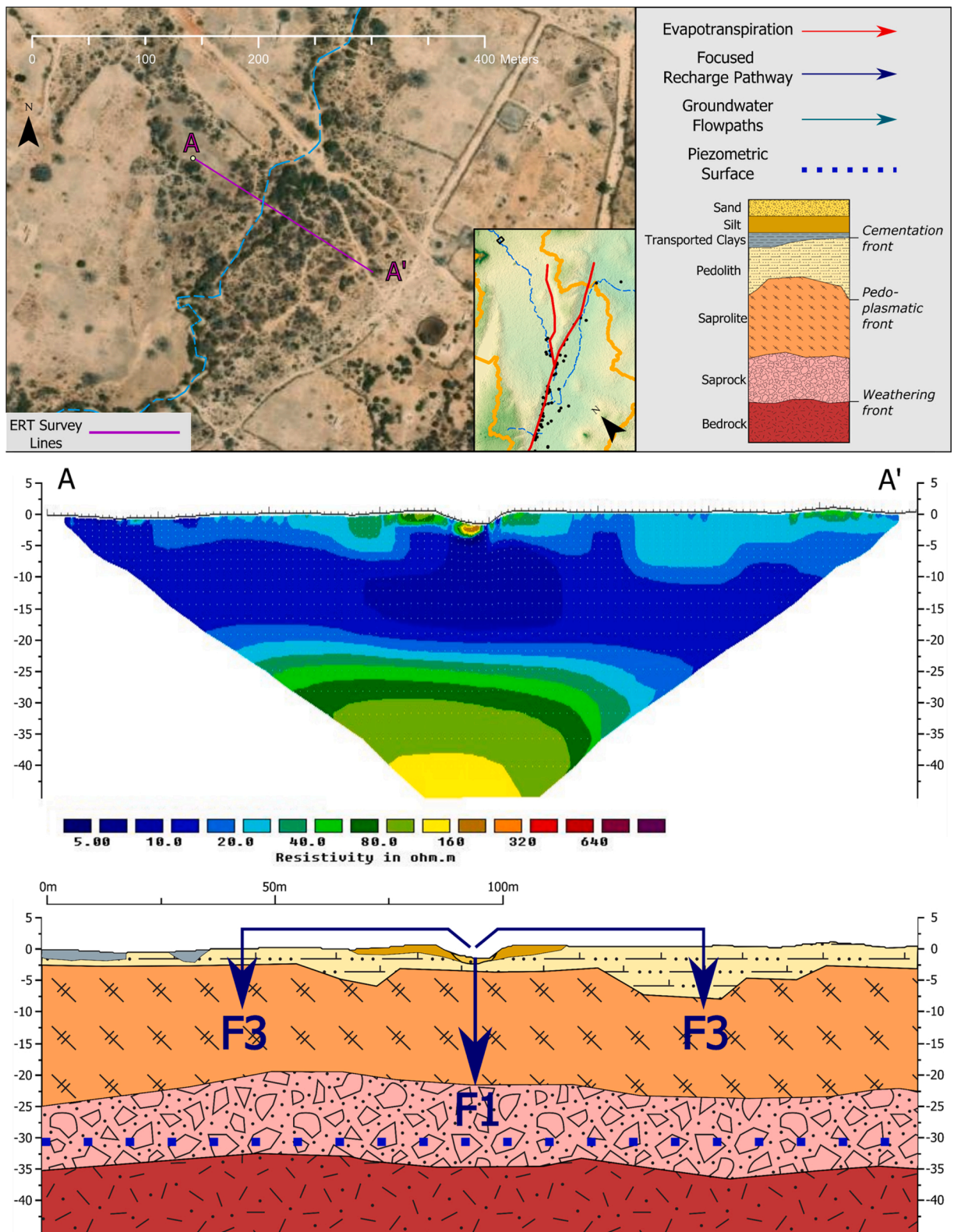


Fig. 5. Meya study site - with map of ERT surveys (top), combined longitudinal geoelectric section of the study site (middle) and interpreted geological structure and conceptual model (bottom). Interpreted borehole logs (Table A2) superimposed in black. Labels and arrows drawn correspond to recharge pathways outlined in Section 3.2.

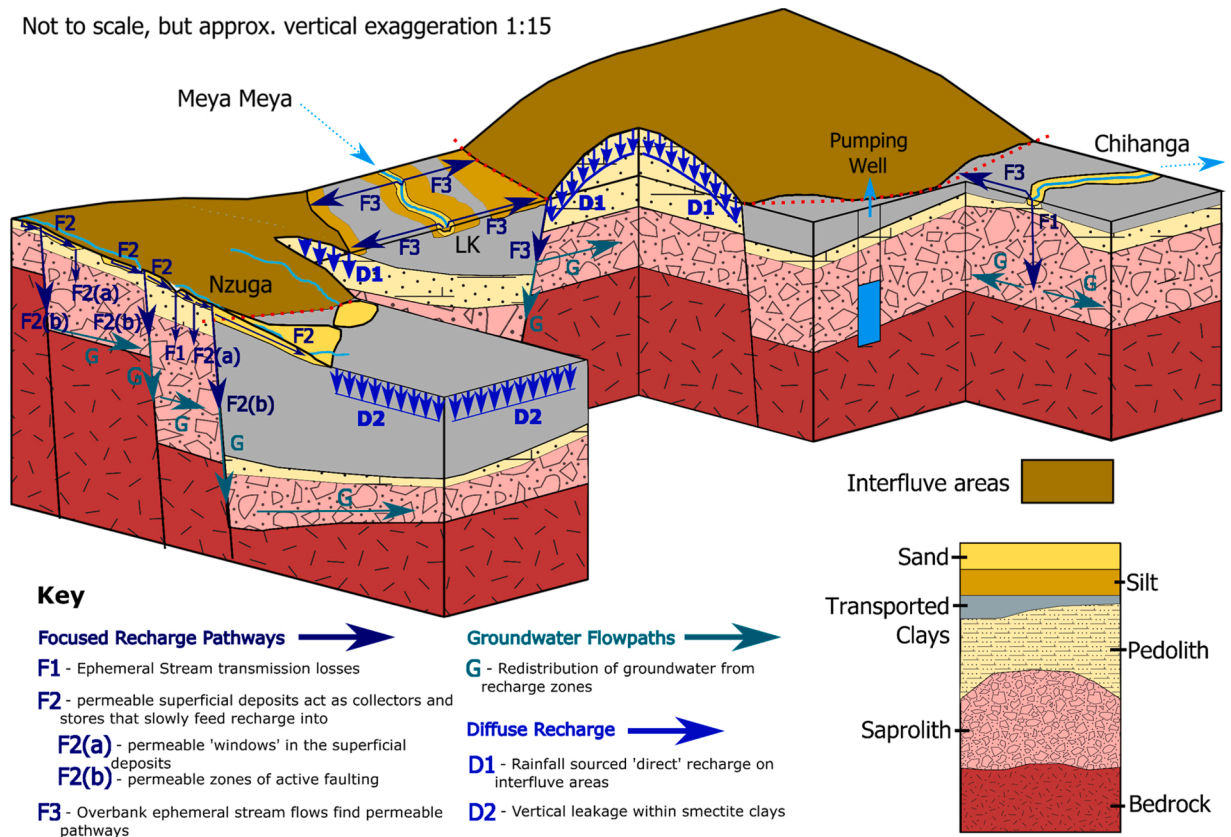


Fig. 6. Conceptual Model of the Makutapora wellfield showing configuration of superficial deposits and highlighting permeable pathways described in Section 3.2. Note that saprock and saprolite horizons have been grouped into 'saprolith' layer.

shallower depths above the water table, variable saturation can lead to micro-weathering environments that create lower pH and higher complexing agent concentrations that accelerate weathering to kaolinite (Dennis et al., 2009; Taylor and Howard, 1999).

At the Nzuga and Meya Meya sites, there is a continuous geoelectric gradient with depth as resistivities further decrease to 10–30 Ω m (Figs. A9–11, A18). Based on interpretation of borehole data, we interpret this as a gradual transition from lower pedolith to upper saprolite zone (d), with a resistivity of 10–30 Ω m typical of saprolites of smectitic composition seen in similar geological provinces (e. g. Pal et al., 1989; Taboada and Garcia, 1999; Robineau et al., 2007; Anudu et al., 2014). This continuous decrease of resistivity is indicative of the boundary between the saprolite and pedolith, known as the pedoplastic front, which is characterized by a change in composition from pedogenic clays to more less weathered, lithic material (Stoops et al., 2018).

However, this 10–30 Ω m saprolitic layer is non-existent in the geoelectric sections at the LK and Chihanga sites (Figs. 4 and 5). Instead, zones of 60–80 Ω m, interpreted as indicative of 1:1 pedolithic clays described earlier, are immediately underlain by higher resistivity zones of 110–450 Ω m, increasing with depth. This higher resistivity zone has been interpreted as zones of fractured bedrock or saprock (e) and distinguished from >250 Ω m zones of coarse sand seen at the surface, or saprolite composed of more 1:1 clays, using borehole lithological interpretations. This wide resistivity range of 110–450 Ω m is common in the saprock of crystalline basement systems because of the fractured nature of the saprock - fractures filled with water or decomposed clays from the saprolite create inherent inhomogeneities in the subsurface resistivity (Dewandel et al., 2006; Robineau et al., 2007)

Sharp discontinuities in resistivity seen at the Nzuga (Figs. 3 and A11–12) and LK site (Figs. 4 and A13) are interpreted as zones of normal faulting and correspond to the Mlemu and Kitope faults, respectively. These discontinuities also correspond with zones of faulting identified from the DEM (see Section 2.2.3) and are typically bounded on the downthrown side with infill of transported clays (i.e. layer b) in Figs. 3 and 4.

Sharp discontinuities in resistivity seen at the Nzuga (Figs. 3 and A11–12) and LK site (Figs. 4 and A13) are interpreted as zones of normal faulting and correspond to the Mlemu and Kitope faults, respectively. These discontinuities also correspond with zones of faulting identified from the DEM (see Section 2.2.3) and are typically bounded on the downthrown side with infill of transported clays (i.e. layer b) in Figs. 3 and 4.

3.2. Conceptual models

Based on the results and interpretation of the geoelectric data collected in the study area, a series of local-scale conceptual hydrogeological models of focused recharge at the Nzuga, LK, Chihanga and Meya Meya sites have been produced. These are shown schematically in Figs. 2–5, respectively, with interpreted borehole lithological data superimposed in black (where available) and focused pathways highlighted in dark blue. These local-scale models were then collated, and in conjunction with borehole log information, used to produce a 3D conceptual model of the recharge processes (including diffuse processes) in the Makutapora wellfield,

shown in Fig. 6. Based on these models, we propose that the superficial (transported) deposits control recharge to the deeper bedrock aquifer system as follows:

F. Focused recharge pathways:

- **F1.** Ephemeral streams lose water into the underlying aquifer via sufficiently permeable intervening superficial deposits and/or weathered bedrock material. This potentially occurs at all study sites. Rates of recharge are likely controlled by the hydraulic properties of the underlying geology, in addition to the stream flow frequency and the depth to the water table (Quichimbo et al., 2020). The lithological characteristics of smectitic Mbuga clays (Fig. 4 and Fig. A1 4) suggest these have low matrix hydraulic conductivities of the order of $1e-10 \text{ ms}^{-1}$, although that could be enhanced by one or two orders of magnitude if preferential flow pathways are prevalent (Crane et al., 2015; Timms et al., 2018). Conversely, streams on the Nzuga, Chihanga and Meya Meya sites (Figs. 2, 4 and 5, respectively) directly overlie pedolitic soils, which are assumed to be more hydraulically conductive. The presence of thick layers of smectite clay rich saprolite underlying this pedolith at the Nzuga and Meya Meya sites however would restrict flow.
- **F2.** Shallow permeable alluvial deposits collect ephemeral stream losses and runoff but due to the variable permeability of underlying materials, this water is stored and slowly redistributed in the subsurface. These shallow stores of water form local perched aquifer systems upstream of the Mlemu fault in the Nzuga site (Shindo, 1990), and within pockets of thick alluvium in the overbank regions of the Little Kinyungwe River at LK (observed in the field by the authors). Such groundwater may flow slowly longitudinally downslope via connected alluvial ribbons to:
 - o **ET.** discharge back to the atmosphere via evaporation either directly, where shallow enough, or through transpiration from riparian vegetation
 - o **F2(a).** flow into the deeper bedrock aquifer via more permeable ‘windows’ in the underlying superficial deposits or
 - o **F2(b)** flow into the deeper bedrock aquifer via highly permeable fractures or fault zones interconnected to the underlying aquifer system (Bense et al., 2013)
- **F3.** Overbank ephemeral stream flows find permeable recharge pathways. Long term stream stage and groundwater relationships suggest that anomalously large rainfall events (and, as such, stream discharges) associated with El Niño events provide significant recharge to the Makutapora wellfield (Seddon et al., 2021). The Little Kingusyngwe River, the main ephemeral stream that channels surface runoff to the wellfield, is often underlain by impermeable smectitic clays (Fig. 3). However, stream stage data indicate these large rainfall events lead to overbank flows, and these flows may locate permeable pathways and faulted zones that bypass this impermeable clay and lead to greater groundwater recharge (Seddon et al., 2021). This recharge pathway is similar to the results of Lange (2005), who also found greater transmission losses with higher flow events attributed mainly to enhanced water losses in flooded overbank areas.

D. Diffuse recharge:

- **D1.** Rainfall-sourced ‘direct’ (‘diffuse’) recharge occurs when soil moisture deficits are overcome, or preferential flow pathways are activated through sufficiently permeable superficial deposits. One previously described mechanism which may be prevalent on the interfluvial areas is enhanced recharge in the vicinity of abundant abandoned termite mounds (Shindo, 1990).
- **D2.** Vertical leakage through smectite clay deposits may be induced or increased by pumping in the underlying aquifer. Although the matrix hydraulic conductivity of the smectite clays are likely to be very low (see pathway F1), biological and weathering processes may compromise the hydraulic integrity of such deposits and allow more permeable syn-depositional macropores to accumulate deep into the formation and act as preferential flow networks (Crane et al., 2015; Timms et al., 2018). This recharge flux via the lowland Mbuga clay may be low, but should not be discounted as a potential pathway for diffuse recharge into the bedrock aquifer system as it may occur over substantial areas.

G. Redistribution of groundwater from recharge zones to the wellfield:

- High transmissivities in the faulted bedrock allow for quick redistribution of groundwater within the fractured aquifer system, capturing recharge from a wide range from the above pathways across the catchment. Pumping tests in the Makutapora Wellfield indicate transmissivities of 400 to $4000 \text{ m}^2 \cdot \text{d}^{-1}$, much greater than typical weathered crystalline rock aquifer systems, that commonly range from 1 to $10 \text{ m}^2 \cdot \text{d}^{-1}$ (Bianchi et al., 2020). These anomalously high transmissivities arise from extensive faulting within the saprock (Maurice et al., 2019; Nkotagu, 1996). These fault systems in essence act as ‘collectors’ for groundwater recharged and stored in the regolith and weathered zone from both focused and diffuse sources as described.

3.3. Discussion and implications

In our study, the use of ERT has enabled a range of geometrical relationships to be defined among different geoelectric layers. The use of outcrop observations and borehole log information has then enabled lithological interpretations to be made from the geoelectric layers. At the Meya Meya site, borehole information was not available and robust lithological interpretations from the ERT data were only possible through the resistivity ranges of subsurface layers ascertained from the other study sites in the catchment, together with outcrop observations within the streambed of the Little Kinyungwe River at Meya Meya (Fig. A1). As such, the borehole logs and outcrop observations were critical to reducing the uncertainty in the conceptual models developed, and caution should be applied

when interpreting ERT data in isolation in such environments.

Our study was not designed to quantitatively determine the relative proportions of diffuse and focused recharge in the study site, but to identify potential recharge typologies. Our conceptual models reveal several potential focused recharge pathways that are consistent with previous studies where residence time indicators have suggested local recharge at Makutapora has a strong component of preferential flow following high-intensity rainfall events (Hayashi and Chiba, 1994; Maurice et al., 2019; Onodera et al., 1995; Senguji, 1999; Shindo, 1990), and with the findings of Taylor et al., 2013a, 2013b and Cuthbert et al., 2019b, which demonstrated that recharge at Makutapora occurs episodically following intensive precipitation, on average two or three times each decade over the last 60 years. This bias of recharge towards intensive precipitation has previously been indicated in hydrometric (Cuthbert et al., 2019b; Taylor et al., 2013b), stable isotope (Banks et al., 2020; Jasechko and Taylor, 2015; Vogel and Van Urk, 1975) and modelling (Eilers et al., 2007) studies in other semi-arid areas. As such, as projected decreases in mean annual precipitation are thought to lead to decreases in groundwater recharge in drylands (Jiménez Cisneros et al., 2014), increases in episodic recharge from more intensive precipitation events may offset these projections. However, caution is needed in such interpretations in the absence of local data on the exact nature of the recharge mechanisms, since local geological heterogeneity can in some cases lead to results that are contrary to this general expectation (Acworth et al., 2020).

The Nzuga study site was specifically chosen to represent smaller headwater streams that drain upper pediplain regions into the wellfield depression. Although these streams drain only 25 % of the catchment area into the wellfield depression, our conceptual model from the Nzuga site (Fig. 3) indicates that these streams may activate a greater proportion of recharge pathways than even the larger Little Kinyasungwe River, which is hypothesized to generate substantial recharge only in large precipitation events that lead to overbank flows (see Section 3.2). Therefore, while the Little Kinyasungwe River may be important in facilitating large recharge events, it may be possible that smaller streams provide a proportion of recharge in years between larger events by slowly 'drip feeding' recharge into the fault system.

As the population of Dodoma and other cities in drylands are set to increase the demand for freshwater in the coming decades (UN, 2017), it is possible that this increased abstraction may lead to increased recharge in the study area. This may occur as increased pumping, and subsequent drawdown, leads to increased capture (Bredehoeft, 2002; Theis, 1940) as the cone of depression reaches further out. For example, this may increase the subsurface storage available in areas of previously shallow water table, thus activating new recharge pathways to collect recharge from an even wider area that may have otherwise been rejected. This increased recharge is difficult to quantify however, and future groundwater level monitoring at a wider range of distances from the wellfield may further elucidate the relative magnitude of diffuse recharge processes in our study site, and its uncertain relationship to focused recharge.

We propose that our study site acts as an analogue for the geological and climatological conditions in many other parts of sub-Saharan Africa, 40 % of which are also underlain by weathered crystalline aquifers (MacDonald et al., 2012). These aquifers provide a vital source of reliable freshwater to over a quarter of a billion people in sub-Saharan Africa (Macdonald et al., 2008; Taylor and Tindimugaya, 2011), and groundwater abstraction to supply domestic water is expected to increase dramatically in the region (Braune and Xu, 2010; Taylor et al., 2009). Furthermore, indirect recharge from ephemeral streams (e.g. pathways F1, F2(a) and F2(b) described in Section 3.2) are likely prevalent in dryland alluvial settings of large global extent where ephemeral streams comprise >80 % of the dryland river network (Levick et al., 2008; Sabater and Tockner, 2009), and there is a growing body of literature using near-surface geophysics to that highlight the importance transmission losses and groundwater recharge in such dryland systems (e.g. Callegary et al., 2007; Shanafield et al., 2020). Our study sites were chosen to represent a range of ephemeral stream geomorphologies observed in dryland regions (Sutfin et al., 2014), excluding bedrock headwater channels which were difficult to access in our study region. Moreover, our models are directly applicable to dryland areas dominated by smectite clay (Acworth and Timms, 2003; Crane et al., 2015; Timms et al., 2019), the presence of which is typical of dryland regions across the world in mafic geological contexts (Oakes and Thorp, 1951).

Accurate quantification of recharge in dryland settings remains a challenge, with no widely applicable method currently available that can directly and accurately quantify the volume of rainwater that reaches the water table (Healy and Scanlon, 2010; Scanlon et al., 2002; Shanafield and Cook, 2014) despite multiple lines of evidence (Villeneuve et al., 2015). We believe our models provide a first step towards the quantification of recharge in drylands by shedding light on potential focused recharge pathways in the region which could be tested in the future using a variety of hydrogeological techniques. For example, soil moisture profiles placed proximal to areas of potential recharge have enabled the tracking of deeper infiltration through multiple layers of varying geological characteristics in hyper-arid settings (Dahan et al., 2008). Temperature tracing has also been used with great success to quantify shallow surface-groundwater interactions beneath ephemeral streams (Rau et al., 2017)

Our models provide an informed physical basis for future 3D numerical modelling of groundwater flow by incorporating superficial geological structure (Turner et al., 2015), and predicting responses to groundwater systems with variable geology to anthropogenic pressures and environmental change (Acworth et al., 2020). Further, our study provides a basis for improved understanding and management of the groundwater system in the Makutapora Wellfield, and opens the door for improved efficacy and implementation of Managed Aquifer Recharge (MAR) in the future by providing a physical basis for recharge in the region (Dillon et al., 2019).

4. Conclusions

Few studies have made detailed observations of superficial geological structure in dryland regions. The use of the ERT method in conjunction with borehole logs and outcrop observations has enabled delineation of a variety of geometries and inter-relationships of superficial geology at four sites in the Makutapora wellfield, Tanzania. These data have revealed lithologies and weathering profiles typical of tropical soils underlain by crystalline basement, and permitted development of conceptual models that outline the role of

superficial deposits in providing multiple potential pathways for focused groundwater recharge that bypass the low permeability smectite clay deposits that cover the wellfield. These can be summarized as follows:

- 1) Superficial sand deposits act as collectors and stores that slowly feed recharge into zones of active faulting.
- 2) These fault zones provide permeable pathways enabling greater recharge to occur and rapid redistribution of recharge.
- 3) Windows within layers of smectitic clay underlying ephemeral streams may provide pathways for focused recharge via transmission losses.
- 4) Overbank flooding during high intensity precipitation events that inundate a greater area of the catchment, increases the probability of activating such permeable pathways.

Our study was not designed to quantitatively determine the relative proportions of diffuse and focused recharge in the study site but does inform future monitoring at a more diverse range of locations within, and peripheral to, the Makutapora wellfield that may further elucidate the relative magnitude of diffuse and focused recharge processes. Specifically, further monitoring of smaller streams such as is expected to understand better and estimate the overall water balance.

The conceptual models we have developed provide a first step for improved understanding of groundwater recharge in drylands by providing a physical basis for how superficial geology controls recharge pathways and processes. These are critical to further understand and quantify for the purpose of improving groundwater management in response to climate and anthropogenic changes.

Author statement

All persons who meet authorship criteria are listed as authors, and all authors certify that they have participated sufficiently in the work to take public responsibility for the content, including participation in the concept, design, analysis, writing, or revision of the manuscript. Furthermore, each author certifies that this material or similar material has not been and will not be submitted to or published in any other publication before its appearance in the Journal of Hydrology: Regional Studies.

Declaration of Competing Interest

The authors report no declarations of interest.

Acknowledgments

Emanuel Zarate is supported by a NERC GW4+ Doctoral Training Partnership studentship from the Natural Environment Research Council [NE/L002434/1] and is thankful for the support and additional funding from CASE partner, the BGS.

The contributions of the BGS authors (MacDonald, Swift and Chambers) are published with the permission of the Director of the BGS.

Further funding is gratefully acknowledged as follows: RGT - *GroFutures* (NE008932/1) under the NERC-ESRC DFID UPGro programme; JK - *GroFutures* (NE008592/1) under the NERC-ESRC DFID UPGro programme; MOC - NERC Independent Research Fellowship (NE/P017819/1).

We are grateful to the support of COSTECH for field permits, and the Tanzanian Ministry of Water for crucial help in the field, Catherine Mwihambo and Lister Kongola in particular.

Appendix A. Supplementary data¹

Supplementary material related to this article can be found, in the online version, at doi:<https://doi.org/10.1016/j.ejrh.2021.100833>.

References

- Abel, C., Horion, S., Tagesson, T., De Keersmaecker, W., Seddon, A.W.R., Abdi, A.M., Fensholt, R., 2020. The human–environment nexus and vegetation–rainfall sensitivity in tropical drylands. *Nat. Sustain.* 4 (1), 25–32. <https://doi.org/10.1038/s41893-020-00597-z>.
- Acworth, R.I., Timms, W.A., 2003. Hydrogeological investigation of mud-mound springs developed over a weathered basalt aquifer on the Liverpool Plains, New South Wales, Australia. *Hydrogeol. J.* 11, 659–672.
- Acworth, R.I., Rau, G.C., Cuthbert, M.O., Jensen, E., Leggett, K., 2016. Long-term spatio-temporal precipitation variability in arid-zone Australia and implications for groundwater recharge. *Hydrogeol. J.* 24, 905–921. <https://doi.org/10.1007/s10040-015-1358-7>.
- Acworth, R.I., Rau, G.C., Cuthbert, M.O., Leggett, K., Andersen, M.S., 2020. Runoff and focused groundwater-recharge response to flooding rains in the arid zone of Australia. *Hydrogeol. J.* 1–28.
- Aizebeokhai, A.P., Singh, V.S., 2013. Field evaluation of 3D geo-electrical resistivity imaging for environmental and engineering studies using parallel 2D profiles. *Curr. Sci.* 504–512.

¹ We are currently awaiting the DOI of the data repository, and will add this to this section when it is sent.

- Andersen, M.S., Acworth, R.I., 2009. Stream-aquifer interactions in the Maules Creek catchment, Namoi Valley, New South Wales, Australia. *Hydrogeol. J.* 17, 2005–2021. <https://doi.org/10.1007/s10040-009-0500-9>.
- Anudu, G.K., Essien, B.I., Obriki, S.E., 2014. Hydrogeophysical investigation and estimation of groundwater potentials of the Lower Palaeozoic to Precambrian crystalline basement rocks in Keffi area, north-central Nigeria, using resistivity methods. *Arab. J. Geosci.* 7, 311–322.
- Banks, E.W., Cook, P.G., Owor, M., Okullo, J., Kebede, S., Nedaw, D., Mleta, P., Fallas, H., Gooddy, D., MacAllister, D.J., et al., 2020. Environmental tracers to evaluate groundwater residence times and water quality risk in shallow unconfined aquifers in sub-Saharan Africa. *J. Hydrol.* 125753.
- Barongo, J.O., Palacky, G.J., 1991. Investigations of electrical properties of weathered layers in the Yala area, western Kenya, using resistivity soundings. *Geophysics* 56, 133–138.
- Beauvais, A., Ritz, M., Parisot, J.-C., Dukhan, M., Bantsimba, C., 1999. Analysis of poorly stratified lateritic terrains overlying a granitic bedrock in West Africa, using 2-D electrical resistivity tomography. *Earth Planet. Sci. Lett.* 173, 413–424.
- Belle, P., Lachassagne, P., Mathieu, F., Barbet, C., Brisset, N., Gourry, J.-C., 2019. Characterization and location of the laminated layer within hard rock weathering profiles from electrical resistivity tomography: implications for water well siting. *Geol. Soc. Lond. Spec. Publ.* 479, 187–205.
- Bense, V.F., Gleeson, T., Loveless, S.E., Bour, O., Scibek, J., 2013. Fault zone hydrogeology. *Earth-Sci. Rev.* 127, 171–192.
- Berdugo, M., Delgado-Baquerizo, M., Soliveres, S., Hernández-Clemente, R., Zhao, Y., Gaitán, J.J., Gross, N., Saiz, H., Maire, V., Lehman, A., Rillig, M.C., Solé, R.V., Maestre, F.T., 2020. Global ecosystem thresholds driven by aridity. *Science (80-)* 367, 787–790. <https://doi.org/10.1126/science.aay5958>.
- Bianchi, M., MacDonald, A.M., Macdonald, D.M.J., Asare, E.B., 2020. Investigating the productivity and sustainability of weathered basement aquifers in tropical Africa using numerical simulation and global sensitivity analysis. *Water Resour. Res.* 56 e2020WR027746.
- Bianconi, F., Borshoff, J., 1984. *Surficial Uranium Occurrences in the United Republic of Tanzania*.
- Binley, A., Hubbard, S.S., Huisman, J.A., Revil, A., Robinson, D.A., Singha, K., Slater, L.D., 2015. The emergence of hydrogeophysics for improved understanding of subsurface processes over multiple scales. *Water Resour. Res.* 51, 3837–3866. <https://doi.org/10.1002/2015WR017016>.
- Braune, E., Xu, Y., 2010. The role of ground water in sub-Saharan Africa. *Ground Water* 48, 229–238. <https://doi.org/10.1111/j.1745-6584.2009.00557.x>.
- Bredehoeft, J.D., 2002. The water budget myth revisited: why hydrogeologists model. *Ground Water* 40, 340–345. <https://doi.org/10.1111/j.1745-6584.2002.tb02511.x>.
- Brunet, P., Clément, R., Bouvier, C., 2010. Monitoring soil water content and deficit using Electrical Resistivity Tomography (ERT) – a case study in the Cevennes area. *France. J. Hydrol.* 380, 146–153. <https://doi.org/10.1016/J.JHYDROL.2009.10.032>.
- Calgarey, J.B., Leenhouts, J.M., Paretto, N.V., Jones, C.A., 2007. Rapid estimation of recharge potential in ephemeral-stream channels using electromagnetic methods, and measurements of channel and vegetation characteristics. *J. Hydrol.* 344, 17–31. <https://doi.org/10.1016/j.jhydrol.2007.06.028>.
- Chen, C., Park, T., Wang, X., Piao, S., Xu, B., Chaturvedi, R.K., Fuchs, R., Brovkin, V., Ciais, P., Fensholt, R., Tømmervik, H., Bala, G., Zhu, Z., Nemani, R.R., Myneni, R. B., 2019. China and India lead in greening of the world through land-use management. *Nat. Sustain.* 2, 122–129. <https://doi.org/10.1038/s41893-019-0220-7>.
- Cherlet, M., Hutchinson, C., Reynolds, J., Hill, J., Sommer, S., von Maltitz, G., 2018. *World Atlas of Desertification*. World Atlas Desertif.
- Clifford, J., Binley, A., 2010. Geophysical characterization of riverbed hydrostratigraphy using electrical resistance tomography. *Near Surf. Geophys.* 8, 493–501.
- Costa, A.C., Bronstert, A., de Araújo, J.C., 2012. A channel transmission losses model for different dryland rivers. *Hydrol. Earth Syst. Sci. Discuss.* 16, 1111–1135. <https://doi.org/10.5194/hess-16-1111-2012>.
- Crane, R.A., Cuthbert, M.O., Timms, W., 2015. The use of an interrupted-flow centrifugation method to characterise preferential flow in low permeability media. *Hydrol. Earth Syst. Sci. Discuss.* 19, 3991–4000.
- Cuthbert, M.O., Mackay, R., Tellam, J.H., Barker, R.D., 2009. The use of electrical resistivity tomography in deriving local-scale models of recharge through superficial deposits. *Q. J. Eng. Geol. Hydrogeol.* 42, 199–209. <https://doi.org/10.1144/1470-9236/08-023>.
- Cuthbert, M.O., Acworth, R.I., Andersen, M.S., Larsen, J.R., McCallum, A.M., Rau, G.C., Tellam, J.H., 2016. Understanding and quantifying focused, indirect groundwater recharge from ephemeral streams using water table fluctuations. *Water Resour. Res.* 52, 827–840. <https://doi.org/10.1002/2015WR017503>.
- Cuthbert, M.O., Gleeson, T., Moosdorf, N., Befus, K.M., Schneider, A., Hartmann, J., Lehner, B., 2019a. Global patterns and dynamics of climate-groundwater interactions. *Nat. Clim. Change* 9, 137–141. <https://doi.org/10.1038/s41558-018-0386-4>.
- Cuthbert, M.O., Taylor, R.G., Favreau, G., Todd, M.C., Shamsudduha, M., Villholth, K.G., MacDonald, A.M., Scanlon, B.R., Kotchoni, D.O.V., Vouillamoz, J.-M., Lawson, F.M.A., Adjomayi, P.A., Kashaigili, J., Seddon, D., Sorensen, J.P.R., Ebrahim, G.Y., Owor, M., Nyenje, P.M., Nazoumou, Y., Goni, I., Ousmane, B.L., Sibanda, T., Ascott, M.J., Macdonald, D.M.J., Agyekum, W., Koussoubé, Y., Wanke, H., Kim, H., Wada, Y., Lo, M.-H., Oki, T., Kukuric, N., 2019b. Observed controls on resilience of groundwater to climate variability in sub-Saharan Africa. *Nature* 572, 230–234. <https://doi.org/10.1038/s41586-019-1441-7>.
- Dahan, O., Tatarsky, B., Enzel, Y., Kulls, C., Seely, M., Benito, G., 2008. Dynamics of flood water infiltration and ground water recharge in Hyperarid Desert. *Ground Water* 46, 450–461. <https://doi.org/10.1111/j.1745-6584.2007.00414.x>.
- Dahlin, T., Wisén, R., Zhang, D., 2007. 3D effects on 2D resistivity imaging—modelling and field surveying results. *Near Surface 2007-13th EAGE European Meeting of Environmental and Engineering Geophysics* p. cp-30.
- Dawson, J.B., 2008. *The Gregory Rift Valley and Neogene-Recent Volcanoes of Northern Tanzania*.
- De Pauw, E.F., Magoggo, J.P., Niemeyer, W., 1983. *Soil Survey Report of Dodoma Capital City District*.
- Dennis, P.G., Hirsch, P.R., Smith, S.J., Taylor, R.G., Valsami-Jones, E., Miller, A.J., 2009. Linking rhizoplane pH and bacterial density at the microhabitat scale. *J. Microbiol. Methods* 76, 101–104.
- DESA, U.N., 2017. *World Population Prospects, the 2017 Revision: Comprehensive Tables, Vol. I*. New York United Nations Dep. Econ. Soc. Aff.
- Dewandel, B., Lachassagne, P., Wyns, R., Maréchal, J.C., Krishnamurthy, N.S., 2006. A generalized 3-D geological and hydrogeological conceptual model of granite aquifers controlled by single or multiphase weathering. *J. Hydrol.* 330 (1–2), 260–284. <https://doi.org/10.1016/j.jhydrol.2006.03.026>.
- Dillon, P., Stuyfzand, P., Grischek, T., Lluria, M., Pyne, R.D.G., Jain, R.C., Bear, J., Schwarz, J., Wang, W., Fernandez, E., et al., 2019. Sixty years of global progress in managed aquifer recharge. *Hydrogeol. J.* 27, 1–30.
- DUWASA, 2017. *Needs, Production and Water Supply*.
- Edwards, L.S., 1977. A modified pseudosection for resistivity and IP. *Geophysics* 42, 1020–1036.
- Eilers, V.H.M., Carter, R.C., Rushton, K.R., 2007. A single layer soil water balance model for estimating deep drainage (potential recharge): an application to cropped land in semi-arid North-east Nigeria. *Geoderma* 140, 119–131. <https://doi.org/10.1016/j.geoderma.2007.03.011>.
- Fawley, A.P., 1958. *Evaporation Rate at Dodoma, Tanganyika*.
- Flinchum, B.A., Banks, E., Hatch, M., Batelaan, O., Peeters, L.J.M., Pasquet, S., 2020. Identifying recharge under subtle ephemeral features in a flat-lying semi-arid region using a combined geophysical approach. *Hydrol. Earth Syst. Sci. Discuss.* 24, 4353–4368.
- Fookes, P.G., 1997. *Tropical Residual Soils: A Geological Society Engineering Group Working Party Revised Report*.
- Gleeson, T., Alley, W.M., Allen, D.M., Sophocleous, M.A., Zhou, Y., Taniguchi, M., VanderSteen, J., 2012. Towards sustainable groundwater use: setting long-term goals, backcasting, and managing adaptively. *Ground Water* 50, 19–26. <https://doi.org/10.1111/j.1745-6584.2011.00825.x>.
- Gleeson, T., Cuthbert, M., Ferguson, G., Perrone, D., 2020. Global groundwater sustainability, resources, and systems in the anthropocene. *Annu. Rev. Earth Planet. Sci.* 48, 431–463. <https://doi.org/10.1146/annurev-earth-071719-055251>.
- Gourdol, L., Clément, R., Juilleret, J., Pfister, L., Hissler, C., 2018. Large-scale ERT surveys for investigating shallow regolith properties and architecture. *Hydrol. Earth Syst. Sci. Discuss.* 1–39. <https://doi.org/10.5194/hess-2018-519>.
- Gourry, J.-C., Vermeersch, F., Garcin, M., Giot, D., 2003. Contribution of geophysics to the study of alluvial deposits: a case study in the Val d’Avaray area of the River Loire, France. *J. Appl. Geophys.* 54, 35–49.
- Griffiths, K.J., MacDonald, A.M., Robins, N.S., Merritt, J., Booth, S.J., Johnson, D., McConvey, P.J., 2011. Improving the characterization of Quaternary deposits for groundwater vulnerability assessments using maps of recharge and attenuation potential. *Q. J. Eng. Geol. Hydrogeol.* 44, 49–61.
- Hayashi, M., Chiba, H., 1994. Identification of groundwater components by Cl⁻ and stable isotope signatures: a case study in a semi-arid basin in Tanzania. *Jap. Groundw. Hydrol.* 36, 259–275.

- Head, L., Adams, M., Mcgregor, H.V., Toole, S., 2014. Climate change and Australia. *Wiley Interdiscip. Rev. Clim. Change* 5, 175–197. <https://doi.org/10.1002/wcc.255>.
- Healy, R.W., Scanlon, B.R., 2010. Estimating Groundwater Recharge. Cambridge University Press, Cambridge. <https://doi.org/10.1017/CBO9780511780745>.
- Huang, J., Li, Y., Fu, C., Chen, F., Fu, Q., Dai, A., Shinoda, M., Ma, Z., Guo, W., Li, Z., Zhang, L., Liu, Y., Yu, H., He, Y., Xie, Y., Guan, X., Ji, M., Lin, L., Wang, S., Yan, H., Wang, G., 2017. Dryland climate change: recent progress and challenges. *Rev. Geophys.* 55, 719–778. <https://doi.org/10.1002/2016RG000550>.
- Jasechko, S., Taylor, R.G., 2015. Intensive rainfall recharges tropical groundwaters. *Environ. Res. Lett.* 10 <https://doi.org/10.1088/1748-9326/10/12/124015>.
- Jiménez Cisneros, B.E., Oki, T., Arnell, N.W., Benito, G., Cogley, J.G., Döll, P., Jiang, T., Mwakalila, S.S., Kundzewicz, Z., Nishijima, A., 2014. Freshwater resources, in: *Climate Change 2014 Impacts, Adaptation and Vulnerability: Part A: Global and Sectoral Aspects*, pp. 229–270. <https://doi.org/10.1017/CBO9781107415379.008>.
- Julian, W., Lounsbury, W., Tamura, A., Van Loenen, R., Wright, M.P., 1963. Brief explanation of the geology. Quarter Degree Sheet 134.
- Kabete, J.M., Groves, D.I., McNaughton, N.J., Mruma, A.H., 2012. A new tectonic and temporal framework for the Tanzanian Shield: implications for gold metallogeny and undiscovered endowment. *Ore Geol. Rev.* 48, 88–124.
- Kashaigili, J.J., 2010. Assessment of Groundwater Availability and Its Current and Potential Use and Impacts in Tanzania. Morogoro, Tanzania.
- Kashaigili, J.J., Mashauri, D.A., Abdo, G., 2003. Groundwater management by using mathematical modeling: case of the Makutupora groundwater basin in Dodoma Tanzania. *Botswana J. Technol.* 12 <https://doi.org/10.4314/bjt.v12i1.15342>.
- Kolusu, S.R., Shamsudduha, M., Todd, M.C., Taylor, R.G., Seddon, D., Kashaigili, J.J., Ebrahim, G.Y., Cuthbert, M.O., Sorensen, J.P.R., Villholth, K.G., et al., 2019. The El Niño event of 2015–2016: climate anomalies and their impact on groundwater resources in East and Southern Africa. *Hydrol. Earth Syst. Sci. Discuss.* 23, 1751–1762.
- LaBrecque, D.J., Miletto, M., Daily, W., Ramirez, A., Owen, E., 1996. The effects of noise on Occam's inversion of resistivity tomography data. *Geophysics* 61, 538–548.
- Lange, J., 2005. Dynamics of transmission losses in a large arid stream channel. *J. Hydrol.* 306, 112–126. <https://doi.org/10.1016/j.jhydrol.2004.09.016>.
- Levick, Laine R., Goodrich, David C., Hernandez, Mariano, Fonseca, Julia, Semmens, Darius J., Stromberg, Juliet C., Tluczek, Melanie, Leidy, Scianni, Melissa, Guertin, Phillip D., Kepner, William G., 2008. The ecological and hydrological significance of ephemeral and intermittent streams in the arid and semi-arid American Southwest. Environmental Protection Agency, Office of Research and Development.
- Loke, M.H., 2001. RES1D ver. 1.0. 1-D Resistivity, IP & SIP Inversion and Forward Modeling. Wenner and Schlumberger arrays, User's Manual.
- Loke, M.H., 2002. RES2DMOD Ver. 3.01. Rapid 2D Resist. Forw. Model. Using Finite-difference Finite-elements Method. Geotomo Software. Man.
- Loke, M.H., Acworth, I., Dahlin, T., 2003. A comparison of smooth and blocky inversion methods in 2D electrical imaging surveys. *Explor. Geophys.* 34, 182–187. <https://doi.org/10.1071/EG03182>.
- Macdonald, A.M., Davies, J., Calow, R.C., 2008. African hydrogeology and rural water supply. *Applied Groundwater Studies in Africa*, pp. 127–148.
- MacDonald, A.M., Bonsor, H.C., Dochartaigh, B.É.Ó., Taylor, R.G., 2012. Quantitative maps of groundwater resources in Africa. *Environ. Res. Lett.* 7, 024009 <https://doi.org/10.1088/1748-9326/7/2/024009>.
- Macheyeki, A.S., Delvaux, D., De Batist, M., Mruma, A., 2008. Fault kinematics and tectonic stress in the seismically active Manyara–Dodoma Rift segment in Central Tanzania—implications for the East African Rift. *J. Afr. Earth Sci.* 51, 163–188.
- Maurice, L., Taylor, R.G., Tindimugaya, C., MacDonald, A.M., Johnson, P., Kaponda, A., Owor, M., Sanga, H., Bonsor, H.C., Darling, W.G., et al., 2019. Characteristics of high-intensity groundwater abstractions from weathered crystalline bedrock aquifers in East Africa. *Hydrogeol. J.* 27, 459–474.
- McCallum, A.M., Andersen, M.S., Rau, G.C., Larsen, J.R., Acworth, R.I., 2014. River-aquifer interactions in a semiarid environment investigated using point and reach measurements. *Water Resour. Res.* 50, 2815–2829. <https://doi.org/10.1002/2012WR012922>.
- Meixner, T., Manning, A.H., Stonestrom, D.A., Allen, D.M., Ajami, H., Blasch, K.W., Brookfield, A.E., Castro, C.L., Clark, J.F., Gochis, D.J., Flint, A.L., Neff, K.L., Niraula, R., Rodell, M., Scanlon, B.R., Singha, K., Walvoord, M.A., 2016. Implications of projected climate change for groundwater recharge in the western United States. *J. Hydrol.* 534, 124–138. <https://doi.org/10.1016/j.jhydrol.2015.12.027>.
- Ministry of Water, Eand M., 1976. Report on Hydrological Investigation of Makutupora Basin for Dodoma Capital Water Supply. Dodoma.
- Misrear, B.D.R., Brown, L., Daly, D., 2009. A methodology for making initial estimates of groundwater recharge from groundwater vulnerability mapping. *Hydrogeol. J.* 17, 275–285.
- NASA, METI, AIST, Japan Spacesystems, US/Japan ASTER Science Team, 2019. ASTER Global Digital Elevation Model V003. <https://doi.org/10.5067/ASTER/ASTGTM.003>.
- Nkotagu, H., 1996. Origins of high nitrate in groundwater in Tanzania. *J. Afr. Earth Sci.* 22, 471–478. [https://doi.org/10.1016/0899-5362\(96\)00021-8](https://doi.org/10.1016/0899-5362(96)00021-8).
- Oakes, H., Thorp, J., 1951. Dark-clay soils of warm regions variously called rendzina, black cotton soils, regur, and tirs 1. *Soil Sci. Soc. Am. J.* 15, 347–354.
- Onodera, S., Kitaoka, K., Shindo, S., 1995. Stable isotopic compositions of deep groundwater caused by partial infiltration into the restricted recharge area of a semiarid basin in Tanzania. *Model. Assess. Monit. Groundw. Qual.* 75–83.
- Pal, D.K., Deshpande, S.B., Venugopal, K.R., Kalbande, A.R., 1989. Formation of di-and trioctahedral smectite as evidence for paleoclimatic changes in southern and central Peninsular India. *Geoderma* 45, 175–184.
- Parsekian, A.D., Singha, K., Minsley, B.J., Holbrook, W.S., Slater, L., 2015. Multiscale geophysical imaging of the critical zone. *Rev. Geophys.* 53, 1–26. <https://doi.org/10.1002/2014RG000465>.
- Právělie, R., 2016. Drylands extent and environmental issues. A global approach. *Earth-Science Rev.* 161, 259–278. <https://doi.org/10.1016/j.earscirev.2016.08.003>.
- Quichimbo, E.A., Singer, M.B., Cuthbert, M.O., 2020. Characterising groundwater–surface water interactions in idealised ephemeral stream systems. *Hydrol. Process.* 34, 3792–3806. <https://doi.org/10.1002/hyp.13847>.
- Rau, G.C., Halloran, L.J.S., Cuthbert, M.O., Andersen, M.S., Acworth, R.I., Tellam, J.H., 2017. Characterising the dynamics of surface water-groundwater interactions in intermittent and ephemeral streams using streambed thermal signatures. *Adv. Water Resour.* 107, 354–369. <https://doi.org/10.1016/j.advwatres.2017.07.005>.
- Ritz, M., Parisot, J.-C., Diouf, S., Beauvais, A., Dione, F., Niang, M., 1999. Electrical imaging of lateritic weathering mantles over granitic and metamorphic basement of eastern Senegal, West Africa. *J. Appl. Geophys.* 41, 335–344.
- Robineau, B., Join, J.-L., Beauvais, A., Parisot, J.-C., Savin, C., 2007. Geoelectrical imaging of a thick regolith developed on ultramafic rocks: groundwater influence. *Austrian J. Earth Sci.* 54, 773–781.
- Rulli, M.C., Savioli, A., D'Odorico, P., 2013. Global land and water grabbing. *Proc. Natl. Acad. Sci.* 110 (3), 892–897. <https://doi.org/10.1073/pnas.1213163110>.
- Rwebugisa, R.A., 2008. Groundwater Re-Charge Assessment in the Makutupora Basin, Dodoma, Tanzania. Msc Thesis. International Institute for Geo-Information Science and Earth Observation, Enschede, The Netherlands.
- Sabater, Sergi, Tockner, Klement, 2009. Effects of hydrologic alterations on the ecological quality of river ecosystems. *Water scarcity in the Mediterranean*. Springer, pp. 15–39.
- Scanlon, B.R., Healy, R.W., Cook, P.G., 2002. Choosing appropriate techniques for quantifying groundwater recharge. *Hydrogeol. J.* 10, 18–39. <https://doi.org/10.1007/s10040-001-0176-2>.
- Scanlon, B.R., Keese, K.E., Flint, A.L., Flint, L.E., Gaye, C.B., Edmunds, W.M., Simmers, I., 2006. Global synthesis of groundwater recharge in semiarid and arid regions. *Hydrol. Process.* 20, 3335–3370. <https://doi.org/10.1002/hyp.6335>.
- Seddon, D., 2019. The Climate Controls and Process of Groundwater Recharge in a Semi-Arid Tropical Environment: Evidence From the Makutupora Basin, Tanzania. UCL (University College London).
- Seddon, D., Kashaigili, J.J., Taylor, R.G., Cuthbert, M.O., Mihale, L., Mwimbo, C., MacDonald, A.M., 2021. Groundwater recharge in a dryland environment: evidence from the Makutupora Basin of Tanzania. *J. Hydrol. Reg. Stud.* In this issue.
- Senguji, F.H., 1999. Importance of isotope hydrology techniques in water resources management: a case study of the Makutupora basin in Tanzania. *Proc. Int. Symp. Isot. Tech. Water Resour. Dev. Manag.*

- Shanafield, M., Cook, P.G., 2014. Transmission losses, infiltration and groundwater recharge through ephemeral and intermittent streambeds: a review of applied methods. *J. Hydrol.* 511, 518–529. <https://doi.org/10.1016/j.jhydrol.2014.01.068>.
- Shanafield, M., Gutiérrez-Jurado, K., White, N., Hatch, M., Keane, R., 2020. Catchment-scale characterization of intermittent stream infiltration; a geophysics approach. *J. Geophys. Res. Earth Surf.* 125 e2019JF005330.
- Shindo, S., 1989. Study on the Recharge Mechanism and Development of Groundwater in the Inland Area of Tanzania: Interim Report of Japan-Tanzania Joint Research, 92p. Unpubl. Rep..
- Shindo, S., 1990. Members of Japan-Tanzania Joint Research Project (1990) and (1994) study on the recharge mechanism and development of groundwater in the inland area of Tanzania. *Prog. Rep. Japan-Tanzania Jt. Res.*
- Simmers, I., 2003. Understanding Water in a Dry Environment: Hydrological Processes in Arid and Semi-arid Zones, International Contributions to Hydrogeology: IAH International Association of Hydrogeologists. Underst. Water a Dry Environ. *Hydrol. Process. Arid Semi-Arid Zo.*
- Singha, K., 2017. Geophysics is not a silver bullet, but worth a shot. *Groundwater* 55, 149. <https://doi.org/10.1111/gwat.12495>.
- Stoops, G., Marcelino, V., Mees, F., 2018. Interpretation of Micromorphological Features of Soils and Regoliths. Elsevier.
- Suffin, N.A., Shaw, J., Wohl, E.E., Cooper, D., 2014. A geomorphic classification of ephemeral channels in a mountainous, arid region, southwestern Arizona, USA. *Geomorphology* 221, 164–175. <https://doi.org/10.1016/j.geomorph.2014.06.005>.
- Taboada, T., García, C., 1999. Smectite formation produced by weathering in a coarse granite saprolite in Galicia (NW Spain). *Catena* 35, 281–290.
- Taylor, R., 2014. Hydrology: when wells run dry. *Nature* 516, 179–180. <https://doi.org/10.1038/516179a>.
- Taylor, G., Eggleton, R.A., 2001. No Title. *Regolith Geol. Geomorphol.*
- Taylor, R.G., Howard, K.W.F., 1999. Lithological evidence for the evolution of weathered mantles in Uganda by tectonically controlled cycles of deep weathering and stripping. *Catena* 35, 65–94.
- Taylor, R., Tindimugaya, C., 2011. The impacts of climate change and rapid development on weathered crystalline rock aquifer systems in the humid tropics of sub-Saharan Africa: evidence from south-western Uganda. *Climate Change Effects on Groundwater Resources: A Global Synthesis of Findings and Recommendations*. CRC Press.
- Taylor, R.G., Koussis, A.D., Tindimugaya, C., 2009. Groundwater and climate in Africa – a review. *Hydrol. Sci. J.* 54, 655–664. <https://doi.org/10.1623/hysj.54.4.655>.
- Taylor, R.G., Scanlon, B., Döll, P., Rodell, M., van Beek, R., Wada, Y., Longuevergne, L., Leblanc, M., Famiglietti, J.S., Edmunds, M., Konikow, L., Green, T.R., Chen, J., Taniguchi, M., Bierkens, M.F.P., MacDonald, A., Fan, Y., Maxwell, R.M., Yecheili, Y., Gurdak, J.J., Allen, D.M., Shamsudduha, M., Hiscock, K., Yeh, P.J.-F., Holman, I., Treidel, H., 2013a. Ground water and climate change. *Nat. Clim. Change* 3, 322–329. <https://doi.org/10.1038/nclimate1744>.
- Taylor, R.G., Todd, M.C., Kongola, L., Maurice, L., Nahozya, E., Sanga, H., MacDonald, A.M., 2013b. Evidence of the dependence of groundwater resources on extreme rainfall in East Africa. *Nat. Clim. Change* 3, 374–378. <https://doi.org/10.1038/nclimate1731>.
- Telvari, A., Cordery, I., Pilgrim, D., 1998. Relations between transmission losses and bed alluvium in an Australian arid zone stream. *Hydrol. Change Environ.* 2, 361–366.
- Theis, C.V., 1940. The source of water derived from wells: essential factors controlling the response of an aquifer to development. *Bridge Eng.* 10, 277–280.
- Timms, W.A., Acworth, R.I., Crane, R.A., Arns, C.H., Arns, J.-Y., McGeeney, D.E., Rau, G.C., Cuthbert, M.O., 2018. The influence of syndepositional macropores on the hydraulic integrity of thick alluvial clay aquitards. *Water Resour. Res.* 54, 3122–3138.
- Timms, W., Whelan, M., Acworth, I., McGeeney, D., Bouzalakos, S., Crane, R., McCartney, J., Hartland, A., 2019. A novel centrifuge permeameter to characterize flow through low permeability strata. In: *ICPMG2014-Physical Modelling in Geotechnics: Proceedings of the 8th International Conference on Physical Modelling in Geotechnics 2014 (ICPMG2014)*. Perth, Australia, 14–17 January 2014, p. 193.
- Turner, R.J., Mansour, M.M., Dearden, R., Dochartaigh, B.É.Ó., Hughes, A.G., 2015. Improved understanding of groundwater flow in complex superficial deposits using three-dimensional geological-framework and groundwater models: an example from Glasgow, Scotland (UK). *Hydrogeol. J.* 23, 493–506.
- UN, 2017. United Nations 2010-2020 Decade for Deserts and the Fight Against Desertification.
- Villeneuve, S., Cook, P.G., Shanafield, M., Wood, C., White, N., 2015. Groundwater recharge via infiltration through an ephemeral riverbed, central Australia. *J. Arid Environ.* 117, 47–58. <https://doi.org/10.1016/j.jaridenv.2015.02.009>.
- Vogel, J.C., Van Urk, H., 1975. Isotopic composition of groundwater in semi-arid regions of southern Africa. *J. Hydrol.* 25, 23–36. [https://doi.org/10.1016/0022-1694\(75\)90036-0](https://doi.org/10.1016/0022-1694(75)90036-0).
- Wada, Y., van Beek, L.P.H., van Kempen, C.M., Reckman, J.W.T.M., Vasak, S., Bierkens, M.F.P., 2010. Global depletion of groundwater resources. *Geophys. Res. Lett.* 37 <https://doi.org/10.1029/2010GL044571> n/a-n/a.
- Wada, Y., van Beek, L.P.H., Wanders, N., Bierkens, M.F.P., 2013. Human water consumption intensifies hydrological drought worldwide. *Environ. Res. Lett.* 8, 034036. <https://doi.org/10.1088/1748-9326/8/3/034036>.
- Wade, F.B., Oates, F., 1938. An Explanation of Degree Sheet No. 52 (Dodoma). *Short Pap.* 17, 52-60.
- Wang, P., Pozdniakov, S.P., Vasilevskiy, P.Y., 2017. Estimating groundwater-ephemeral stream exchange in hyper-arid environments: field experiments and numerical simulations. *J. Hydrol.* 555, 68–79. <https://doi.org/10.1016/j.jhydrol.2017.10.004>.
- Wheater, H., Sorooshian, S., Sharma, K.D., Kapil, D., 2008. *Hydrological Modelling in Arid and Semi-Arid Areas*. Cambridge University Press.
- Wheater, H., Mathias, S., Li, X., 2010. Groundwater modelling in arid and semi-arid areas. *Groundwater Modelling in Arid and Semi-Arid Areas*. <https://doi.org/10.1017/CBO9780511760280>.
- WMO, 2020. World Weather Information Service [WWW Document]. URL. <http://worldweather.wmo.int/en/city.html?cityId=667>.
- Wright, E.P., Burgess, W.G., 1992. *The Hydrogeology of Crystalline Basement Aquifers in Africa*. Hydrogeol. Cryst. Basement Aquifers Africa.